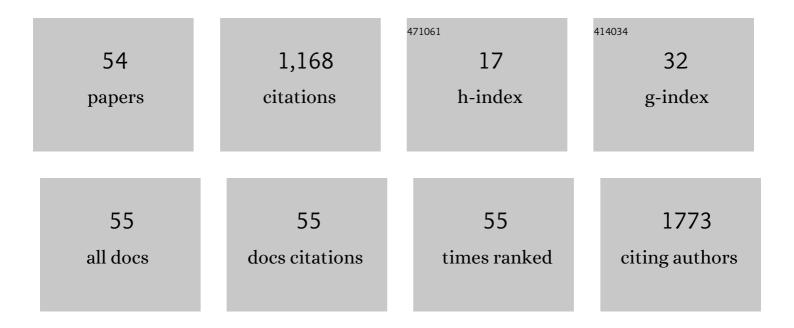
Sébastien Mulé

List of Publications by Year in descending order

Source: https://exaly.com/author-pdf/5696303/publications.pdf

Version: 2024-02-01



<u> <u>SÃ</u> Ωβλςτιένι Μιμ ÃΩ</u>

#	Article	IF	CITATIONS
1	Predicting Survival After Hepatocellular Carcinoma Resection Using Deep Learning on Histological Slides. Hepatology, 2020, 72, 2000-2013.	3.6	158
2	Retention of Plasmodium falciparum ring-infected erythrocytes in the slow, open microcirculation of the human spleen. Blood, 2008, 112, 2520-2528.	0.6	141
3	Multiphase Liver MRI for Identifying the Macrotrabecular-Massive Subtype of Hepatocellular Carcinoma. Radiology, 2020, 295, 562-571.	3.6	88
4	Advanced Hepatocellular Carcinoma: Pretreatment Contrast-enhanced CT Texture Parameters as Predictive Biomarkers of Survival in Patients Treated with Sorafenib. Radiology, 2018, 288, 445-455.	3.6	84
5	Noninvasive Contrast-enhanced US Quantitative Assessment of Tumor Microcirculation in a Murine Model: Effect of Discontinuing Anti-VEGF Therapy. Radiology, 2010, 254, 420-429.	3.6	62
6	Hepatocellular carcinoma: CT texture analysis as a predictor of survival after surgical resection. European Radiology, 2019, 29, 1231-1239.	2.3	47
7	Metastatic melanoma: pretreatment contrast-enhanced CT texture parameters as predictive biomarkers of survival in patients treated with pembrolizumab. European Radiology, 2019, 29, 3183-3191.	2.3	36
8	Applications of dual energy computed tomography in abdominal imaging. Diagnostic and Interventional Imaging, 2016, 97, 593-603.	1.8	35
9	Can dual-energy CT replace perfusion CT for the functional evaluation of advanced hepatocellular carcinoma?. European Radiology, 2018, 28, 1977-1985.	2.3	34
10	An automatic respiratory gating method for the improvement of microcirculation evaluation: application to contrast-enhanced ultrasound studies of focal liver lesions. Physics in Medicine and Biology, 2011, 56, 5153-5165.	1.6	29
11	Regularized Estimation of Contrast Agent Attenuation to Improve the Imaging of Microbubbles in Small Animal Studies. Ultrasound in Medicine and Biology, 2008, 34, 938-948.	0.7	27
12	Neuroendocrine tumors of the small bowel: evaluation with MR-enterography. Clinical Imaging, 2016, 40, 541-547.	0.8	27
13	Prognostic value of anthropometric measures extracted from whole-body CT using deep learning in patients with non-small-cell lung cancer. European Radiology, 2020, 30, 3528-3537.	2.3	27
14	MDCT Linear and Volumetric Analysis of Adrenal Glands: Normative Data and Multiparametric Assessment. European Radiology, 2016, 26, 2494-2501.	2.3	24
15	Advances in radiological imaging of gastrointestinal tumors. Critical Reviews in Oncology/Hematology, 2009, 69, 153-167.	2.0	23
16	Quantitative correlation between uptake of Gd-BOPTA on hepatobiliary phase and tumor molecular features in patients with benign hepatocellular lesions. European Radiology, 2018, 28, 4243-4253.	2.3	23
17	Immune Profiling of Combined Hepatocellular- Cholangiocarcinoma Reveals Distinct Subtypes and Activation of Gene Signatures Predictive of Response to Immunotherapy. Clinical Cancer Research, 2022, 28, 540-551.	3.2	23
18	Whole-Body Functional MRI and PET/MRI in Multiple Myeloma. Cancers, 2020, 12, 3155.	1.7	22

#	Article	IF	CITATIONS
19	lso- or hyperintensity of hepatocellular adenomas on hepatobiliary phase does not always correspond to hepatospecific contrast-agent uptake: importance for tumor subtyping. European Radiology, 2019, 29, 3791-3801.	2.3	19
20	Primary rectal cancer local staging. Diagnostic and Interventional Imaging, 2014, 95, 485-494.	1.8	18
21	Hepatobiliary MR contrast agent uptake as a predictive biomarker of aggressive features on pathology and reduced recurrence-free survival in resectable hepatocellular carcinoma: comparison with dual-tracer 18F-FDG and 18F-FCH PET/CT. European Radiology, 2020, 30, 5348-5357.	2.3	17
22	Correlation and Agreement Between Contrast-Enhanced Ultrasonography and Perfusion Computed Tomography forÂAssessment of Liver Metastases from Endocrine Tumors:ÂNormalization Enhances Correlation. Ultrasound in Medicine and Biology, 2012, 38, 953-961.	0.7	16
23	Imaging of the postoperative liver: review of normal appearances and common complications. Abdominal Imaging, 2015, 40, 2761-2776.	2.0	16
24	Prediction of overall survival in patients with hepatocellular carcinoma treated with Y-90 radioembolization by imaging response criteria. Diagnostic and Interventional Imaging, 2021, 102, 35-44.	1.8	16
25	Intrahepatic immune changes after hepatitis c virus eradication by directâ€acting antiviral therapy. Liver International, 2020, 40, 74-82.	1.9	14
26	Myosteatosis as an independent risk factor for mortality after kidney allograft transplantation: a retrospective cohort study. Journal of Cachexia, Sarcopenia and Muscle, 2022, 13, 386-396.	2.9	14
27	Measurement variability of liver metastases from neuroendocrine tumors on different magnetic resonance imaging sequences. Diagnostic and Interventional Imaging, 2018, 99, 73-81.	1.8	12
28	CT texture analysis as a predictor of favorable response to anti-PD1 monoclonal antibodies in metastatic skin melanoma. Diagnostic and Interventional Imaging, 2022, 103, 97-102.	1.8	12
29	Contrast-enhanced ultrasound after devascularisation of neuroendocrine liver metastases: functional and morphological evaluation. European Radiology, 2013, 23, 805-815.	2.3	10
30	Classification of Segmental Wall Motion in Echocardiography Using Quantified Parametric Images. Lecture Notes in Computer Science, 2005, , 477-486.	1.0	8
31	Current imaging of rectal cancer. Clinics and Research in Hepatology and Gastroenterology, 2015, 39, 168-173.	0.7	8
32	Predictors of mortality following emergency open colectomy for ischemic colitis: a single-center experience. World Journal of Emergency Surgery, 2020, 15, 40.	2.1	8
33	Optimization of whole-body 2-[18F]FDG-PET/MRI imaging protocol for the initial staging of patients with myeloma. European Radiology, 2021, , 1.	2.3	8
34	Fast T2-weighted liver MRI: Image quality and solid focal lesions conspicuity using a deep learning accelerated single breath-hold HASTE fat-suppressed sequence. Diagnostic and Interventional Imaging, 2022, 103, 479-485.	1.8	8
35	Detection of aneurysmal subarachnoid hemorrhage 3â€months after initial bleeding: evaluation of T2* and FLAIR MR sequences at 3â€T in comparison with initial non-enhanced CT as a gold standard. Journal of NeuroInterventional Surgery, 2016, 8, 813-818.	2.0	7
36	Registration and functional analysis of CT dynamic image sequences for the follow-up of patients with hepatic tumors undergoing antiangiogenic therapy. Irbm, 2010, 31, 263-270.	3.7	6

#	Article	IF	CITATIONS
37	Virtual unenhanced imaging of the liver derived from 160-mm rapid-switching dual-energy CT (rsDECT): Comparison of the accuracy of attenuation values and solid liver lesion conspicuity with native unenhanced images. European Journal of Radiology, 2020, 133, 109387.	1.2	6
38	An Original Methodology for Quantitative Assessment of Perfusion in Small Animal Studies Using Contrast-Enhanced Ultrasound. Annual International Conference of the IEEE Engineering in Medicine and Biology Society, 2007, 2007, 347-50.	0.5	5
39	Sinusoidal obstruction syndrome: a warning about autologous stem cell transplantation preceded by regimens containing oxaliplatin. Bone Marrow Transplantation, 2020, 55, 1834-1836.	1.3	5
40	Impact of the 18F-FDG-PET/MRI on Metastatic Staging in Patients with Hepatocellular Carcinoma: Initial Results from 104 Patients. Journal of Clinical Medicine, 2021, 10, 4017.	1.0	5
41	Acute Biliary Obstruction after Transarterial Radioembolization with Yttrium-90. Journal of Vascular and Interventional Radiology, 2019, 30, 2043-2045.	0.2	4
42	Unusual intestinal and extra intestinal findings in Crohn's disease seen on abdominal computed tomography and magnetic resonance enterography. Clinical Imaging, 2020, 59, 30-38.	0.8	4
43	Utility of Early Posttreatment PET/CT Evaluation Using FDG or 18F-FCH to Predict Response to 90Y Radioembolization in Patients With Hepatocellular Carcinoma. American Journal of Roentgenology, 2021, , .	1.0	4
44	Whole-Body Diffusion-weighted MR Imaging of Iron Deposits in Hodgkin, Follicular, and Diffuse Large B-Cell Lymphoma. Radiology, 2018, 286, 560-567.	3.6	3
45	Evaluation of measurement variability in quantitative analyses: Application to dynamic contrast-enhanced MRI histogram analysis in rectal cancer. Diagnostic and Interventional Imaging, 2018, 99, 421-422.	1.8	2
46	Évaluation par AFSIM d'une méthode régularisée de correction de l'atténuation en imagerie c contraste ultrasonore. Irbm, 2009, 30, 174-178.	le 3.7	1
47	Sinusoidal Obstruction Syndrom (SOS): Warning about Autologous Stem Cell Transplantation (ASCT) Preceded By Regimens Containing Oxaliplatin. Blood, 2018, 132, 4597-4597.	0.6	1
48	Focal Benign Liver Lesions and Their Diagnostic Pitfalls. Radiologic Clinics of North America, 2022, 60, 755-773.	0.9	1
49	Sinusoidal Obstruction Syndrome: Warning About Autologous Stem Cell Transplantation Preceded by Regimens Containing Oxaliplatin. Clinical Lymphoma, Myeloma and Leukemia, 2019, 19, S264-S265.	0.2	0
50	Hypermetabolic bilateral kidney enlargement associated with diffuse large B-cell lymphoma. Lancet Oncology, The, 2021, 22, e81.	5.1	0
51	Clinical, Immunophenotypic and Genetic Characteristics of Aggressive (non-Burkitt) B-Cell Lymphoma in a Real Life Cohort. Blood, 2019, 134, 4122-4122.	0.6	0
52	Integrative Study of a High-Grade B-Cell Lymphoma Cohort of 45 Patients: A Single Institution Real Life Study. Blood, 2021, 138, 4576-4576.	0.6	0
53	Abdominal imaging in ICU patients with viral pneumonia: Are findings in COVID-19 patients really different from those observed with non-SARS-CoV-2 viral pneumonia?. , 2022, 1, 1-5.		0
54	Impact of Extended Use of Ablation Techniques in Cirrhotic Patients with Hepatocellular Carcinoma: A Cost-Effectiveness Analysis. Cancers, 2022, 14, 2634.	1.7	0